Supporting Information for

Supramolecular Alternating Copolymer with Highly Efficient Fluorescence Resonance Energy Transfer

Anwesha Chakraborty, [a] Pradipta Kumar Das, [b] Biman Jana*[b] and Suhrit Ghosh*[a]

[a] School of Applied and Interdisciplinary Sciences; [b] School of Chemical Sciences. Indian Association for the Cultivation of Science, 2A and 2B Raja S. C. Mullick Road, India-700032
Email for corresponding authors: psusg2@iacs.res.in; pcbj@iacs.res.in

Materials and methods: Solvents were purchased from commercial sources (Merck-India) and purified following standard procedures.[1] Synthesis of NDI-1 has been reported elsewhere.[2] Naphthalene di-anhydride, DBH (1,3-Dibromo-5,5-dimethylhydantoin), butane-thiol and glycine were purchased from Sigma Aldrich. Spectroscopy grade solvents were used for physical studies. ^{1}H NMR experiments were performed on a Bruker DPX-500 MHz, 300 MHz NMR instrument and the peaks were calibrated against TMS. For determination of mass of the synthesized compound, electron spray ionization (ESI) technique Q-tof-micro quadruple mass spectrometer was used. UV/Vis spectra were performed in a JASCO-V750 spectrometer. FT-IR spectra were recorded in a Perkin Elmer Spectrum 100FT-IR spectrometer. Atomic force microscopy (AFM) images were taken in an Innova instrument from Bruker. Fluorescence emission spectra were recorded in a FluoroMax-3 spectrophotometer, from Horiba Jobin Yvon. Picosecond-resolved fluorescence transients were measured by using a time-correlated single photon counting setup (Horiba Jobin Yvon IBH) with IRF (instrument response function) = 45 ps, where the sample was excited at 440 nm with an excitation source of NanoLED-440L(pd,200ps). Rheology was

measured using an advanced Rheometer AR 2000 (TA Instrument). PXRD data were recorded on a Bruker D8 advance diffractometer with Cu-Kα radiation (α=0.154 nm). The voltage of 40kV and the current of 40 mA were used, and the data were recorded from 0.5–30.

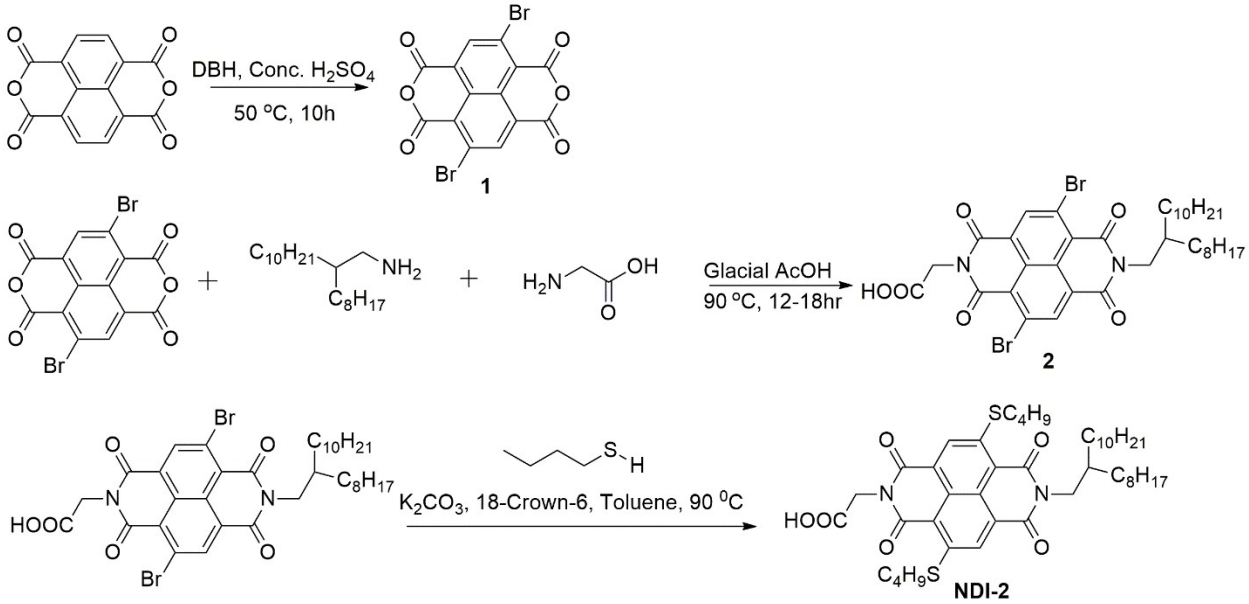

Synthesis of NDI-2: Synthesis of NDI-2 was accomplished in a few steps (Scheme S1).

Scheme S1: Synthetic scheme of NDI-2

Compound 1: Commercially available naphthalene dianhydride (2 g, 7.46 mmol) was taken in a single necked 100 mL round bottom flask and 20 mL of concentrated sulphuric acid added at 0 °C to dissolve it. Then, DBH (1,3-Dibromo-5,5-dimethylhydantoin) (8 g, 27.97 mmol) was added to the reaction mixture in 2 portions over an hour at 0-25 °C. The reaction was stirred at 50 °C for 12 h. Then the reaction mixture was poured into crushed ice when a yellow solid was precipitated. The product was filtered and washed with methanol and used as it is for the next step. Crude yield- 90 %. ^{1}H NMR (400 MHz, DMSO-d_6, ppm): δ = 8.78 (s, 2H); HRMS (ESI): m/z calc. for $C_{14}H_2Br_2O_6$ $[M]^+$: 425.820; found $[M+H]^+$: 425. 830.

Compound 2: 500 mg of compound **1** (1.176 mmol) was first dissolved in 3.0 ml glacial acetic acid. Then 1.05 g of 2-octyl dodecyl amine (3.529 mmol) [2] was added to it and the reaction mixture was stirred at 90 °C for 4 h. By course of this reaction, color of the solution changed from yellow color to straw yellow. Then in the same reaction mixture 310 mg (4.117mmol) of glycine was added and the reaction mixture and stirred for another 24 h. Then the reaction mixture was poured dropwise in water. Sticky precipitate was obtained which was washed with water and little methanol to remove excess acetic acid and then air dried for few hours to get the crude product. The crude product was purified using column chromatography using a solvent gradient ranging from chloroform to 2 % methanol in chloroform to get pure product **2** in 10 % yield. ^{1}H NMR: (300 MHz, DMSO-d_6, ppm): δ = 8.769 (d, 2H), 4.763 (s, 2H), 3.986 (d, 2H), 1.923 (t,1H), 1.197 (s, 32H), 0.838 (t, 6H).

NDI-2: 44 mg of molecule **2** (0.056 mmol), 31 mg of butane thiol (excess, 0.338 mmol), 46 mg (0.338 mmol) of activated K_2CO_3 and 9 mg of 18-Crown-6 (0.0338 mmol) were taken in a single-neck round bottom flask and 5 mL of dry toluene was added to it. The reaction mixture was stirred at 70 ˚C for 24h. After that the excess toluene and unreacted thiol reactant were evaporated and the crude mixture was extracted using water and dichloromethane. The organic layer was collected and evaporated to dryness to get the crude mixture. The crude mixture was then purified using column chromatography with a solvent gradient ranging from chloroform to 1 % methanol in dichloromethane to obtain the pure product as a red solid. Yield: 80 %. ^{1}H NMR: (300 MHz, $CDCl_3$, ppm): δ = 8.684 (s, 2H), 5.004 (s, 2H), 4.145 (d, 2H), 3.222 (q, 4H), 2.041 (t,1H), 1.883 (q, 4H), 1.632 (q,4H), 1.024-1.221 (m, 32H,) 0.884 (t, 6H)., 0.840 (t, 6H). ^{13}C NMR ($CDCl_3$, 400 MHz, TMS): δ (ppm) = 171, 163.59, 162.81, 162.69, 162.20, 149.52, 148.78, 128.67,128.37, 125.23, 124.08, 123.98, 118.42, 76.80, 77.01, 77.22, 45.18, 38.88, 41.18, 36.66, 37.10, 36.48,

33.70, 33.24, 32.76, 32.05, 32.02, 31.93, 31.91, 31.88, 31.60, 31.44, 30.20, 30.17, 30.07, 29.97, 29.91, 29.70, 29.66, 29.63, 29.55, 29.34, 29.30, 29.05, 27.09, 27.32, 26.40, 25.93, 22.66, 22.68, 22.33, 22.30, 14.24.

Sample preparation for supramolecular homopolymers of NDI-1 and NDI-2: Stock solutions of NDI-1 or NDI-2 was prepared in $CHCl_3$ (2.0 mM). Then 50 µL of the stock solution was transferred to a separate vial and $CHCl_3$ was evaporated to obtain solid residue. 500 µL decane was added to the vial to dissolve those residue by sonication and heating so that the final concentration becomes 0.2mM. The solution was kept at room temperature (25-27 ^oC) for about 2-3 h before any spectroscopy (UV/Vis, Fluorescence, FT-IR) or micrsocpoy (AFM) experiments were performed. For AFM experiments, soltuion was drop-casted on the mica surface and images were captured after air drying for 24 h.

Sample preparation for supramolecular copolymer of NDI-1 and NDI-2: 150 µL of each of the stock solutions (1:1 case) or 200 µL of NDI-1 and 100 µL of NDI-2 stock solution (2:1 case), or 100 µL of NDI-1 and 200 µL of NDI-2 stock solution (1:2 case) was transferred to a vial and mixed by mild sonication. Then $CHCl_3$ was evaporated to obtain a solid residue. That solid residue was dissolved in 300 µL decane by sonication and heating and kept at room temperature (25-27 ^oC) when a red gel (total concentration of NDIs = 2.0 mM) was obtained. 50 µL of that gel was taken into a vial and diluted with 450 µL of decane. That solution was used for UV-Vis, fluorescence and TCSPC studies. Same solution was drop-casted on mica surface to check the morphology by AFM. Gel prepared in similar way but at higher concentration like 10mM was used for Micro-DSC and rheological studies.

In a typical cooling experiment, 1:1 NDI-1 + NDI-2 copolymer solution in decane was placed in the UV/Vis spectrophotometer and the temperature was reduced from 80 °C to 25 °C at a rate 2

ºC/min using the in built temperure-controlled programme in the equipment. Spectra were recorded in 2 °C interval. Then mole fraction of aggregate at each temperature was estimated from the absorbance at 561 nm using the following equation (1)

$$\alpha\text{agg} = \frac{A(T) - A(\min)}{A(\max) - A(\min)} \text{----------} (1)$$

A (max), *A* (min) and *A* (T) stand for maximum and minimum absorbance of the band at 561 nm and absorbance at the particular temperature (T), respectively.

Calculation of rate of FRET:

Equations used for the calculation: Rate of energy transfer[3-4] (k_T) depends on the Förster radius (R_0, the distance between the donor and the acceptor at 50% efficiency of energy transfer), the Förster distance (R, distance between the donor and acceptor) and fluorescence lifetime of donor in absence of acceptor, τ_D and calculated using the equation (1)

$$k_T = \frac{1}{\tau_D}\left(\frac{R_0}{R}\right)^6 \text{----------} (1)$$

Förster distance (R) can be calculated using the equation (2)

$$r^6 = \left[R^6(1-E)\right]/E \text{----------}(2)$$

where E is energy transfer efficiency, calculated using the equation, $E = 1 - \frac{\tau_{DA}}{\tau_D}$ -------(3)

(τ_D and τ_{DA} are fluorescence lifetime of donor in absence and presence of acceptor respectively).

Förster radius (R_0) is calculated using the equation (4)

$$R_0 = 0.211 \left(k^2 \eta^{-4} Q_D J(\lambda)\right)^6 \text{----------(4)}$$

Where k^2 is the relative orientation in space of the transition dipoles of the Donor and acceptor (for randomly oriented D and A molecules, assumed value is 2/3), refractive index (η) of medium, fluorescence quantum yield (Q_D) of donor fluorophore and J(λ) is the overlap integral (the quantitative measure of the overlap between the donor emission and acceptor absorption).

J(λ) is calculated using the equation (5)

$$J(\lambda) = \frac{\int_0^\infty F_D(\lambda)\, \varepsilon_A(\lambda)\, \lambda^4}{\int_0^\infty F_D(\lambda) d\lambda} \text{----------(5)}$$

where $F_D(\lambda)$ is the fluorescence intensity of the donor and $\varepsilon_A(\lambda)$ is the extinction coefficient of the acceptor at λ.

Methods and Calculations: First the overlapping integral, J(λ), has been calculated from figure S10a using origin software, the value of which is 8.515×10^{13}. Then quantum yield of the donor, NDI-1 in aggregated state in decane has been calculated using the standard quinine sulphate (in 0.5M H_2SO_4) as their absorption spectra have significant overlap and value obtained with respect to quinine sulphate is 0.12. Putting all those values in equation (3) and considering refractive index (*η)* of decane, 1.412, the Förster radius (R_0) has been calculated and value obtained is 23 Å. Energy transfer efficiency (E) has been calculated using the equation (3) where τ_D and τ_{DA} values 0.46 ns and 0.03 ns, respectively, obtained from fluorescent transients' measurements (TCSPC). Putting the values of R_0 and E in the equation (2), Förster distance (R) has been calculated to be 15 Å.

Finally, rate of energy transfer (k_T) has been calculted using the equation (1) and value obtained is 28 ns^{-1}.

Computational details:

System preparation: To obtain the forcefield parameters for two NDI molecules as well as the decane molecule we have used Automated Topology Builder (ATB version 3.0).[5] All MD simulations for necessary equilibration and production runs as well as analysis were done using Gromacs 2020.6 [6] along with modified gromos54a7 [7] topologies. For visualization purposes, we have used VMD[8] and Pymol.

The individual NDI systems were solvated in decane. We took 40 NDI-1 and added 2500 solvent molecules. This system was minimized using the steepest descent algorithm. We performed a 1ns of NVT equilibration and NPT equilibration each followed by 2 μs of the production run in the NPT ensemble with a timestep of 1 fs. All details regarding the equilibrium simulation have been provided in the Table S1. The equilibrations were done by restraining all of the NDI molecules with a force constant of 1000 $kJ.mol^{-1}nm^{-2}$ while posing no restrictions on the solvent molecules. These processes were repeated for the NDI-2 system (40 NDI-2 in 2500 decane molecules) as well as a 1:1 mixture of NDI-1 and NDI-2 systems (20 NDI-1 and 20 NDI-2 in 2500 decane molecules). The temperature was controlled by coupling to a Nose-Hoover thermostat with a time constant of 0.5 ps. The pressure was maintained using a Berendsen barostat with a time constant of 0.5 ps. All the simulations were performed at 300K temperature. We sorted out the most stable NDI-1, NDI-2, and NDI-1+NDI-2 dimers respectively, solvated each of the dimers in decane solvent, and performed another set of 1.5 μs of the production run. We have found three distinct trimeric

configurations. We observed two distinct trimers as alternate repeating patterns for the oligomers formed in the mixed system i.e., NDI-2+NDI-1+NDI-2 and NDI-2+NDI-1+NDI-1. A combination of NDI-1+NDI-2+NDI-1 was also abundant in the system which was considered to be another repeating analog of NDI-2+NDI-1+NDI-2.

System	Solute (NDI-1)	Solute (NDI-2)	Solvent (n-Decane)	Box-size (after NPT equilibration)	Production run time (ns)
NDI-1	40	0	2500	9.3 nm	2000
NDI-2	40	0	2500	9.3 nm	2000
1:1 Mixed	20	20	2500	9.45 nm	2000
NDI-1	2	0	782	6.2 nm	1500
NDI-2	0	2	893	6.5 nm	1500
1:1 Mixed	1	1	814	6.32 nm	1500

Table S1. System details of all NDI equilibrium simulations

Enhanced sampling techniques: We calculated the stability of the dimers as well as trimers in terms of binding free energy, which was evaluated by the potential of mean force using the umbrella sampling method. For this, we took the most stable dimer from the 1 μs production runs. Our reaction coordinate was the distance between the central ring of two NDI molecules. We have kept one of the NDI molecules restricted to its initial position and allowed to sample the free NDI constrained at a fixed distance using a force constant of 1000 kJ $mol^{-1}nm^{-2}$ away from the surface of the restricted NDI. This constrained distance was gradually increased from 0.25 nm to 2.5 nm with a 0.05 nm increment in each configuration. Each configuration was allowed to sample for 5 ns in the NVT ensemble. The weighted histogram analysis method (WHAM) module from GROMACS was used to obtain the potential of mean force (PMF) profile. We made sure that the distance range was properly sampled by constructing a histogram and checking the overlap between each subsequent configuration to avoid any biased profile.

The trimer obtained from the mixed systems was also analyzed using umbrella sampling. In this case, the first two NDI molecules from each group were constrained in their initial position and the last NDI molecule was allowed to sample freely at defined distances away from the surface of the constrained NDI group. The distance between the constrained NDIs and the free NDI was varied from 0.3 nm to 3 nm with 0.05 nm increment in each configuration and maintained with a force constant of 1000 kJ $mol^{-1}nm^{-2}$. Each configuration was allowed to sample for 5ns in the NVT ensemble. The PMF profile construction was done again using the WHAM module from GROMACS.

Gaussian calculations: In the present quantum mechanical (QM) calculation, all atoms were allowed to move freely during the optimization using the Gaussian G09 package.[9] Each NDI

molecule was optimized at the B3LYP/6-311G(d,p) level of theory. ESP on the surface of NDI molecules was calculated in Mulliken populations with atomic units. Observations explain the presence of a relatively higher negative charge concentration on the central ring of NDI-2 with respect to NDI-1. It can be assumed that this charge difference between NDI-1 and NDI-2 is what gives the leading binding stability between these two which further can be supported by the enthalpic stability gain between the mixed systems. Whereas for individual pair formation, the similar partial relative positive charge or partial relative negative charge gives less stability during binding which further supports these systems' gain of stability through entropic contribution.

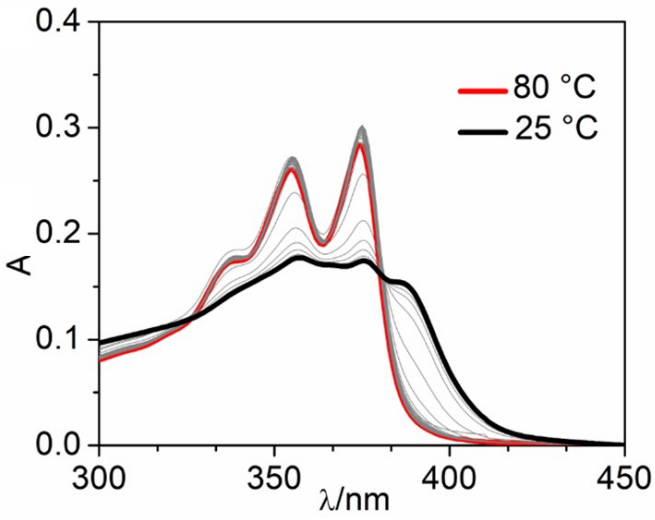

Additional Figures:

Figure S1. Variable temperature UV/Vis spectroscopy data (Cooling from 80 °C to 25 °C at a rate 2°C / min) of NDI-1 in decane. Data interval 2 °C, c = 0.2 mM, l = 0.1cm.

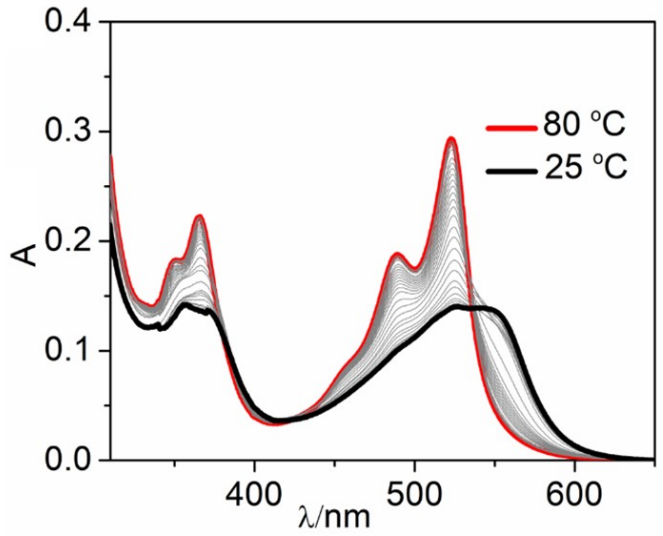

Figure S2. Variable temperature UV/Vis spectroscopy data (Cooling from 80 °C to 25 °C at a rate 2°C / min) of NDI-2 in decane. Data interval 2 °C, c = 0.2 mM, l = 0.1cm

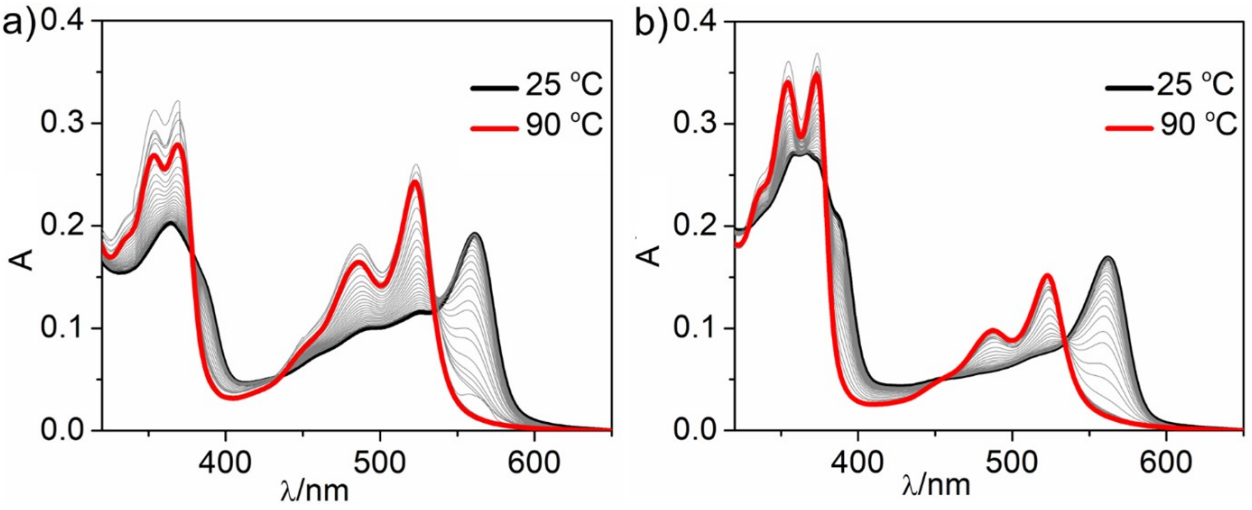

Figure S3. Variable temperature UV/Vis spectroscopy data (heating from 25 °C to 90 °C at a rate 2°C / min) of NDI-1 + NDI-2 mixed samples in decane with a) 1:2 and b) 2:1 ratio of the two monomers. Data interval 2 °C, c = 0.2 mM, l = 0.1cm.

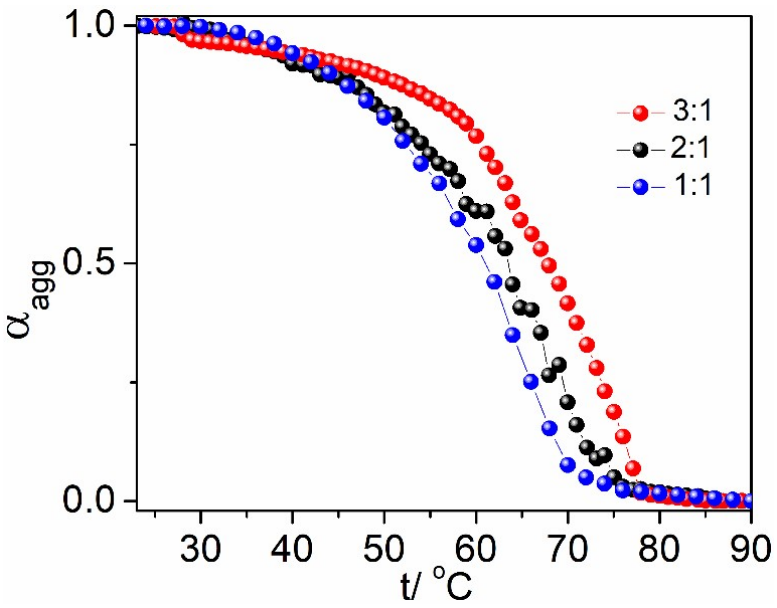

Figure S4. Variation of α_{agg} (calculated from change in intensity at 561 nm) as a function of temperature (heating from 25 °C to 90 °C at a rate 2 ºC/ min, l = 0.1 cm) for the three mixed samples (NDI-2: NDI-1= 1:1, 1:2, 1:3). In each case concentration of NDI-2 was fixed at 0.2 mM and that of NDI-1 varies.

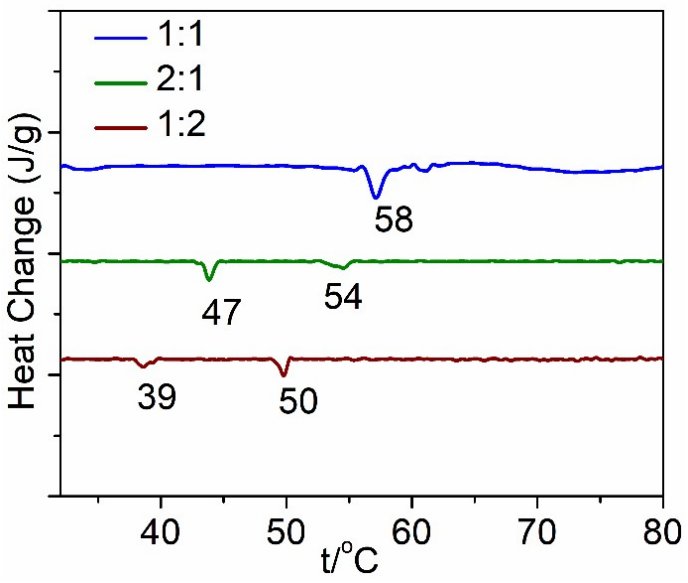

Figure S5. Micro-DSC traces (heating) of 1:1, 2:1 and 1:2 gel in decane (c = 5mM) showing two different phase transition temperatures for 1:2 and 2:1 case. Also the peak for the copolymer appears at lower temperature for samples with stoichiometric imbalance.

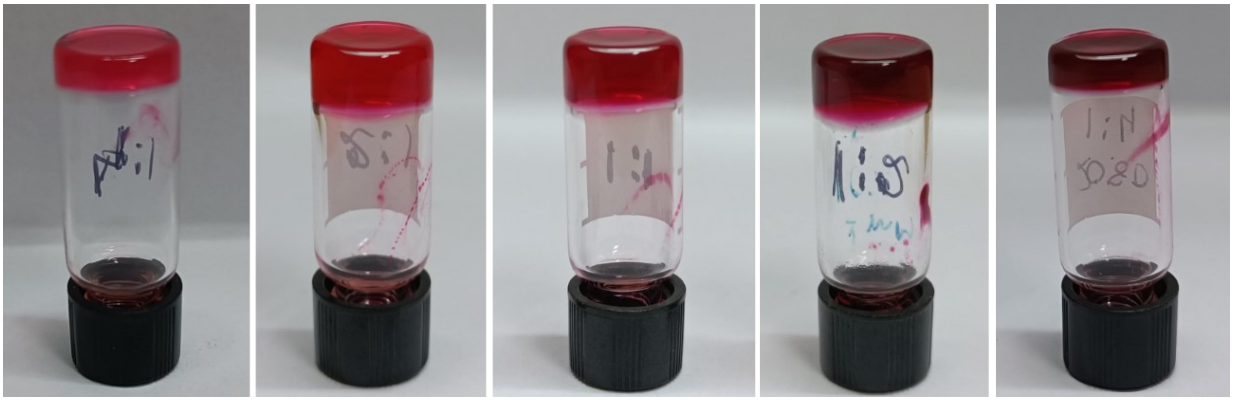

4:1 **2:1** **1:1** **1:2** **1:4**

Figure S6. Images of NDI-1 + NDI-2 mixed gels in decane (c = 2.0 mM). NDI-1/ NDI-2 ratio varies in each vial as indicated by the numbers in the bottom of the gel images.

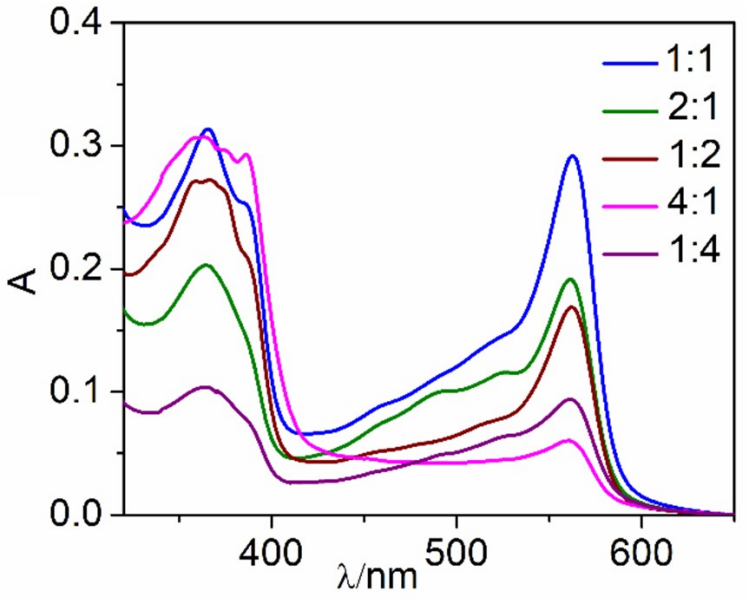

Figure S7. UV/Vis spectra of (NDI-1+ NDI-2) supramolecular copolymer in decane with varying NDI-1/ NDI-2 ratio as indicated in the figure. c = 0.2mM, l = 0.1cm.

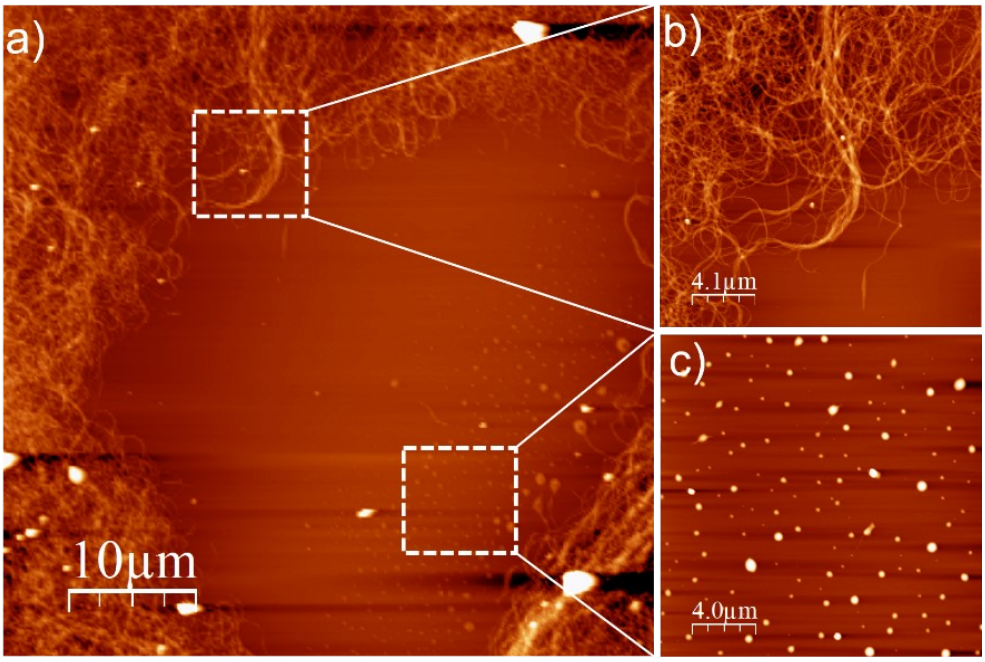

Figure S8. (a) AFM image of the sample prepared from NDI-1 + NDI-2 (1:2) mixture in decane (c = 0.2mM). Zoomed images show co-existence of (b) fibrillar and (c) spherical structures.

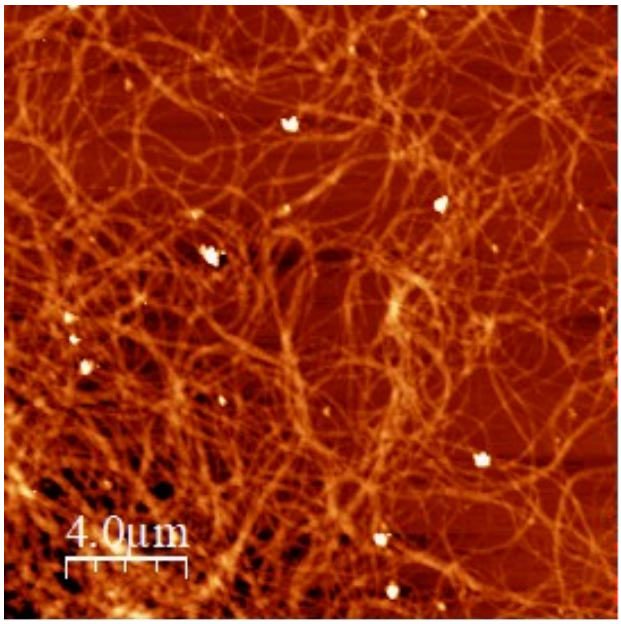

Figure S9. AFM images of the sample prepared from 2:1 mixture of NDI-1 + NDI-2 in decane (c = 0.2mM) showing entangled fibrillar morphology.

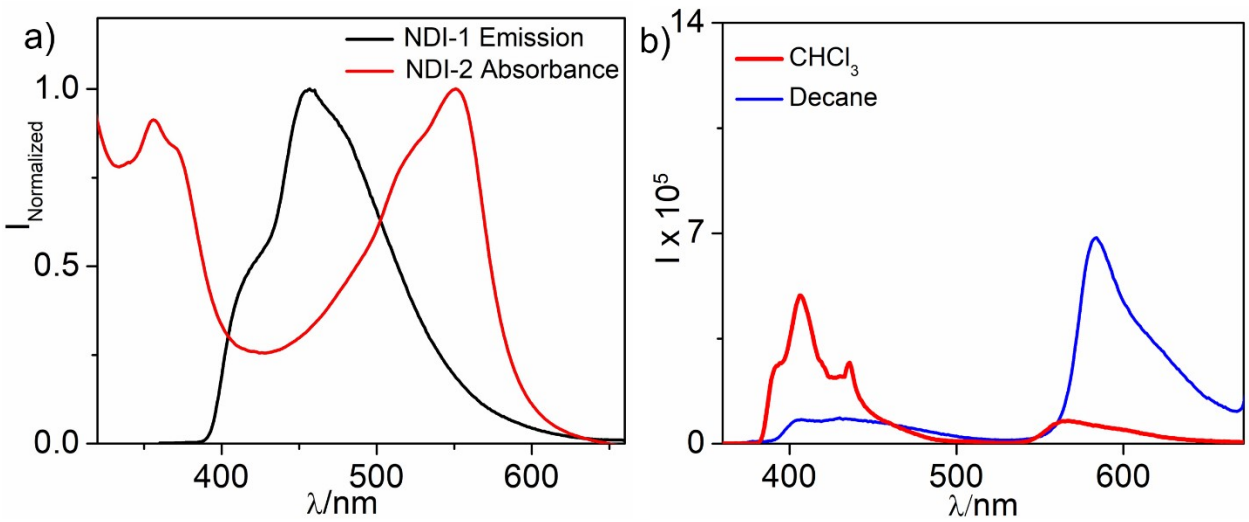

Figure S10. a) Intensity normalized absorption spectrum of NDI-2 (acceptor) and emission spectrum of NDI-1(donor) in decane; b) Emission spectra of 1:1 mixture of NDI-1 and NDI-2 in good solvent, $CHCl_3$ and decane showing no FRET in $CHCl_3$ [c= 0.2mM, l = 0.1cm, λ_{ex} = 360nm].

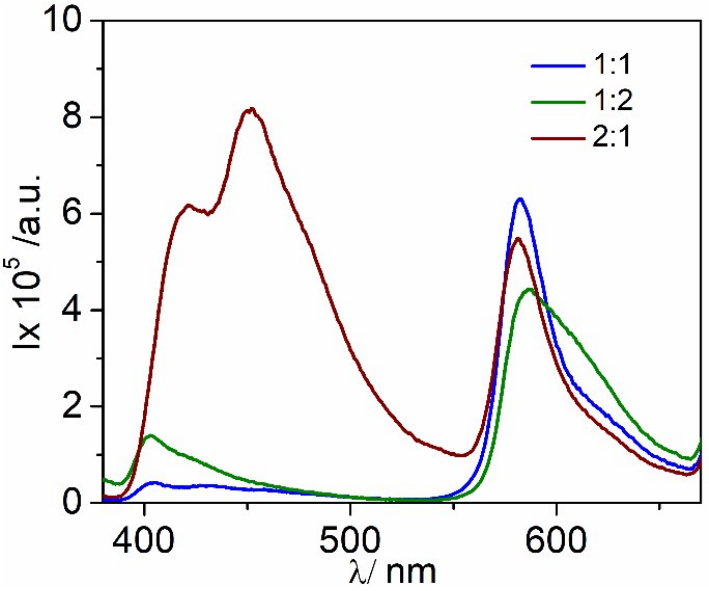

Figure S11. Emission spectra of NDI-1 + NDI-2 mixed samples in decane [c= 0.2mM, l = 0.1cm, λ_{ex} = 360 nm] with varying NDI-1/ NDI-2 ratio as indicated inside the figure.

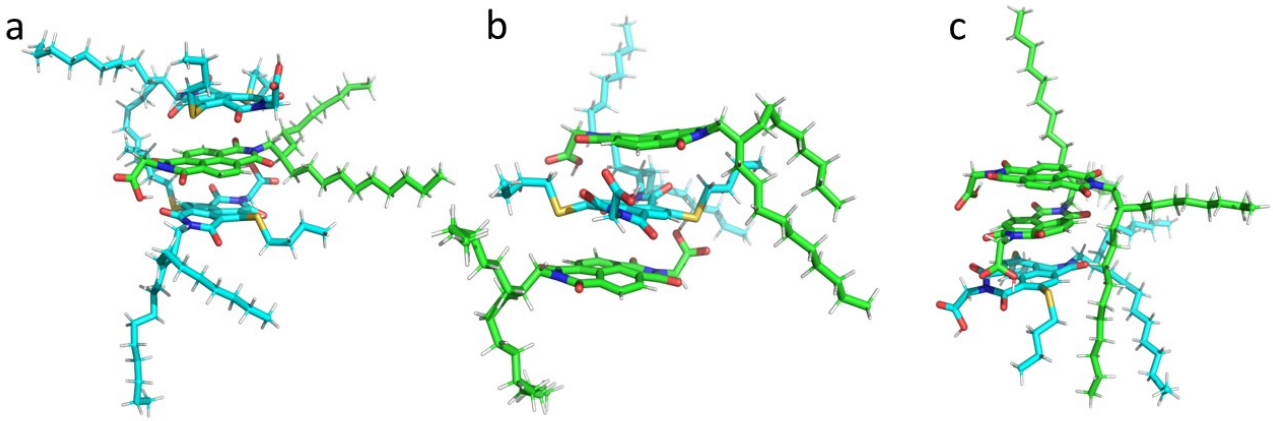

Figure S12. Various trimers obtained from NDI-1+NDI-2 mixed systems, NDI-1 are color-coded by green and NDI-2 are color-coded by cyan color and trimers are named according to their sequence from bottom to top in stacking. a) NDI-2+NDI-1+NDI-2 trimer. b) NDI-1+NDI-2+NDI-1 trimer. c) NDI-2+NDI-1+NDI-1 trimer.

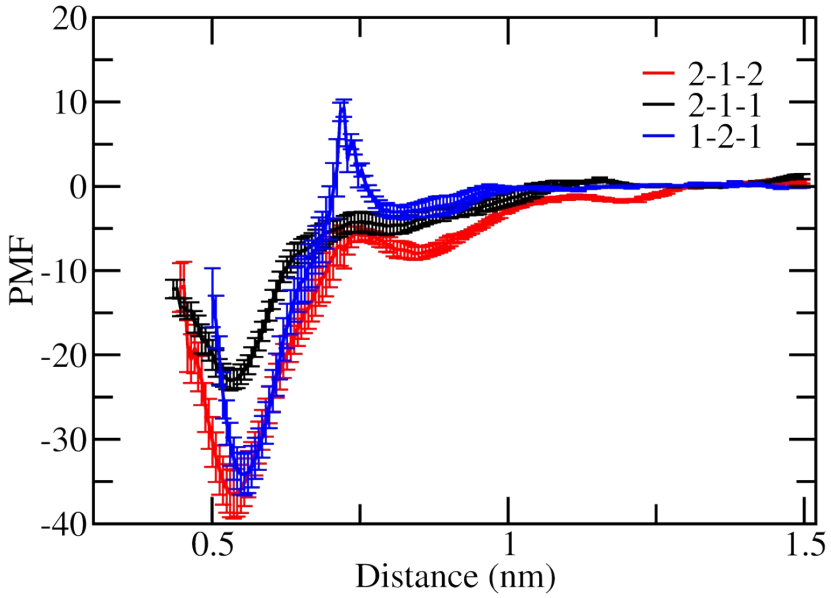

Figure S13. PMF profile of three stable trimers found. 2-1-1 corresponds to NDI-2+NDI-1+NDI-1 trimer defined by the black line, 2-1-2 corresponds to NDI-2+NDI-1+NDI-2 defined by the red line and 1-2-1 corresponds to NDI-1+NDI-2+NDI-1 defined by the blue line.

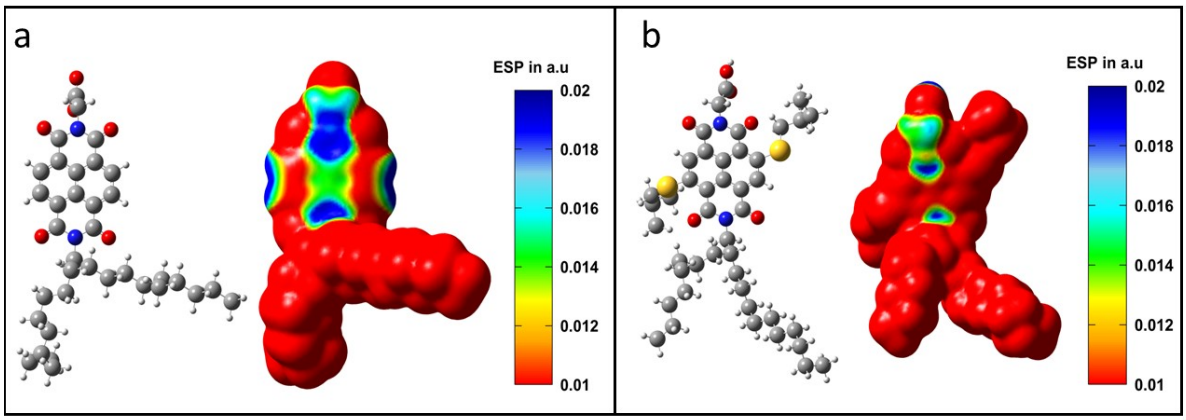

Figure S14. Electrostatic potential on the surface of NDI molecules a) NDI-1 molecule, the left-hand side image is a molecular representation of the molecule, and the right-hand side image shows the electrostatic potential on the surface of the molecule in atomic units. b) NDI-2 molecule, the left-hand side image is a molecular representation of the molecule, and the right-hand side image shows the electrostatic potential on the surface of the molecule in atomic units.

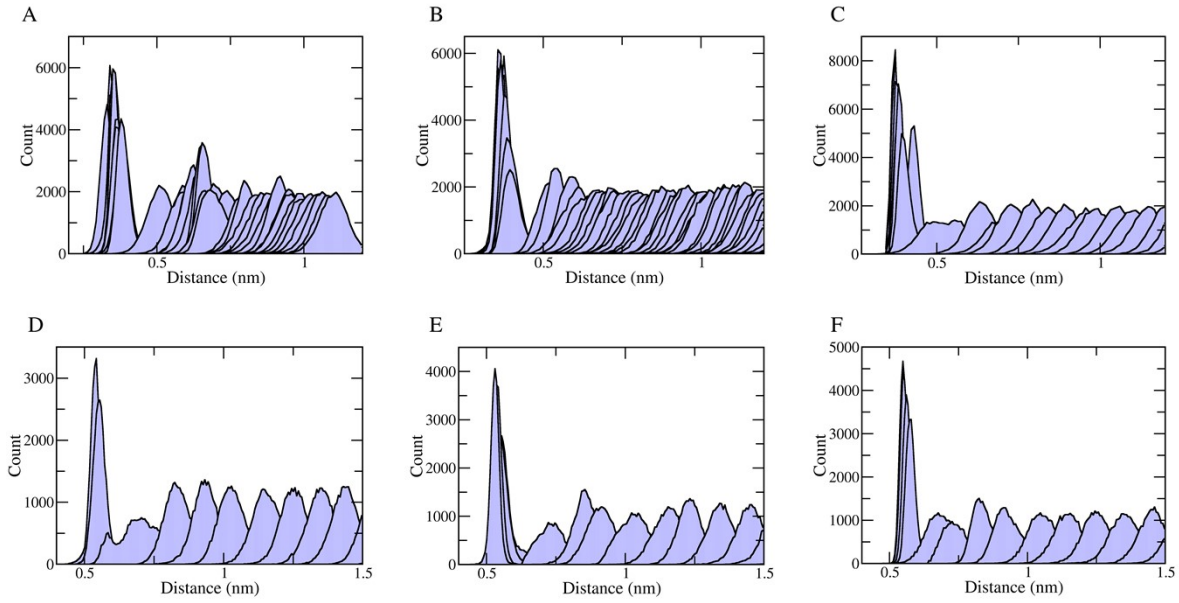

Figure S15: Umbrella sampling histogram overlap between each window. a) NDI-1+NDI-1 dimer, b) NDI-2+NDI-2 dimer, c) NDI-1+NDI-2 dimer, d) NDI-2+NDI-1+NDI-1 trimer, e) NDI-2+NDI-1+NDI-2 trimer, f) NDI-1+NDI-2+NDI-1 trimer.

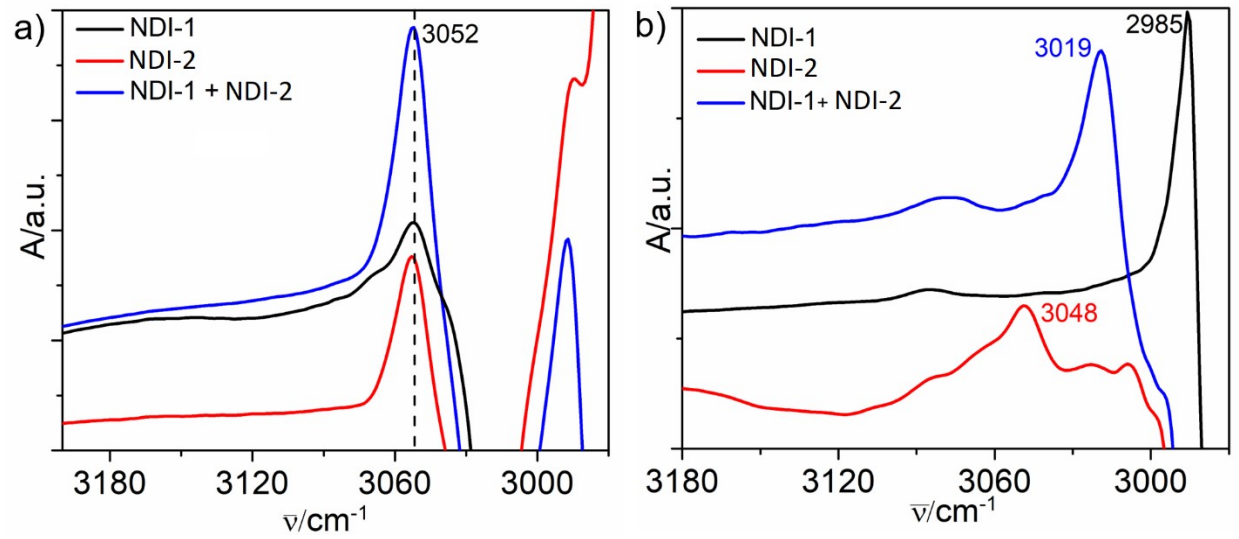

Figure S16. Selected region of the FT-IR spectra of NDI-1 and NDI-2 and their 1:1 mixture in a) $CHCl_3$ and in b) decane [c = 2mM].

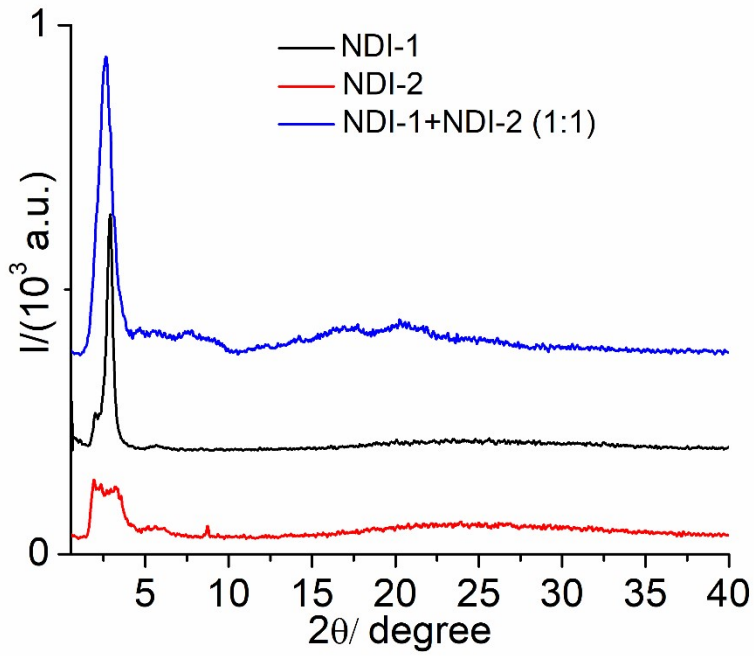

Figure S17. Comparison of the PXRD pattern of NDI-1 and NDI-2 homopolymers and copolymer (NDI-1 + NDI-2).

References:

1. D. Perrin, W. L. F. Armarego, D. R. Perrin, *Purification of Laboratory Chemicals, 2nd Ed., Oxford: Pergamon* 1980.
2. A. Chakraborty, G. Ghosh, D. S. Pal, S. Varghese, S. Ghosh, *Chem. Sci.,* 2019, **10**, 7345.

3. S. M. Müller, H. Galliardt, J. Schneider, B.G. Barisas, T. Seide, *Frontiers in Plant Science*, 2013, *4*, 1-20.
4. P. Rajdev, S. Ghosh, *J. Phys. Chem. B*, 2019, **123,** 327.
5. M. Stroet, B. Caron, K. M. Visscher, D. P. Geerke, A. K. Malde, A. E. Mark, J. Chem. Theory Comput., 2018, 14, 5834.
6. Lindahl; Abraham; Hess; van der Spoel, GROMACS 2020.6 Source Code. Zenodo March 4, 2021.
7. N. Schmid, A. P. Eichenberger, A. Choutko, S. Riniker, M. Winger, A. E. Mark, W. F. van Gunsteren, Eur Biophys J., 2011, 40, 843.
8. W. Humphrey, A. Dalke, K. Schulten, Journal of Molecular Graphics, 1996, 14, 33.
9. M. J. Frisch, H. B. Schlegel, G. E. Scuseria, M. A. Robb, J. R. Cheeseman, G. Scalmani, V. Barone, G. A. Petersson, H. Nakatsuji, X. Li, M. Caricato, A. Marenich, J. Bloino, B. G. Janesko, R. Gomperts, B. Mennucci, H. P. Hratchian, J. V. Ortiz, A. F. Izmaylov, J. L. Sonnenberg, D. Williams-Young, F. Ding, F. Lipparini, F. Egidi, J. Goings, B. Peng, A. Petrone, T. Henderson, D. Ranasinghe, V. G. Zakrzewski, J. Gao, N. Rega, G. Zheng, W. Liang, M. Hada, M. Ehara, K. Toyota, R. Fukuda, J. Hasegawa, M. Ishida, T. Nakajima, Y. Honda, O. Kitao, H. Nakai, T. Vreven, K. Throssell, J. A. Montgomery, J. E. Peralta, F. Ogliaro, M. Bearpark, J. J. Heyd, E. Brothers, K. N. Kudin, V. N. Staroverov, T. Keith, R. Kobayashi, J. Normand, K. Raghavachari, A. Rendell, J. Burant, S. S. Iyengar, J. Tomasi, M. Cossi, J. M. Millam, M. Klene, C. Adamo, R. Cammi, J. W. Ochterski, R. L. Martin, K. Morokuma, O. Farkas, J. B. Foresman, D. J. Fox, Gaussian 09, Revision B.01. Gaussian, Inc.: Wallingford CT, 2010.